Vibration Assessment of Ship Structures

Adrian Constantinescu
ANAST, University of Liege
Liege, Belgium

Alain Nême
EA 4325 - ENSIETA / Université de Brest / ENIB
Brest, France

Philippe Rigo
ANAST, University of Liege
Liege, Belgium

ABSTRACT

Nowadays, noise and vibration problems tend to become an important part of the design process in the naval industry. Vibrations often affect the passengers comfort, but more dangerously may damage the structure, embarked merchandise and equipments. A simple way to avoid vibrations is to prevent the resonance conditions. The paper presents a study about the vibration of local structures (beam structures and stiffened panels) with application in the marine industry. The model has been implemented in FORTRAN into a numerical module and will be integrated in the near future with the LBR-5 generic stiffened structure optimization code.

KEY WORDS: Vibration; natural frequency; resonance; stiffened panel; concentrated mass; Lapack library

INTRODUCTION

Vibrations acting into the mechanical systems can cause many problems at different levels such as mechanical and performance degradation. If we include the human factor, the study of the vibration becomes extremely important.

The main application of this study refers to marine field and particularly to ferries and RO-RO ships for which the vibrational comportment is often verified in the preliminary design stage process or during the structural design phase. A ferry or RO-RO ship is characterized by very large decks that may suffer from fatigue due to vibrations. The LNG's tank walls can be also affected by vibrations, but in this case we must take into account the fluid-structure interaction. Another important application connecting the marine and vehicle fields refers to the dynamics vehicle/ship-deck investigations. The experiences demonstrate that the dynamic interactions between the vehicles and the vessel deck (for example, a roll-on/roll-off RO-RO vessel with vehicle cargo) may be very different from that of static case. It was found that the vehicle cargoes can work as mass dumpers to reduce at least one mode shape response of the deck (Jia, 2004).

The work presented in this paper do not treat the global vibrations of these ships and it is devoted only to local structure, such as beams, stiffened panels, their assemblies, and other connected problems. Thus, in addition of the marine engineering field (decks, ship tanks, offshore structures), this study may be applied in other engineering domains such as automotive or civil construction industries.

For type of structure, the vibration analyses have a dual aim. The first goal is purely theoretical and supposes to determine their natural frequencies. The second aim assumes to measure and compare, during the normal operating, the vibrational characteristics (vibrational displacement, velocity and acceleration) with the agreed limit values because despite careful analysis, vibrations cannot be avoided completely. This paper will not cover these last aspects, but it will give you some general indications to calculate the vibrational magnitudes.

Compared to analytical models, the 3D-FEM models are preferred because almost structural details and mass distribution can be modeled. However, the FE simulations cannot be evermore used in multi-crietria structural optimization design processes due to its very large CPU times. But, today the naval industry has very strict deadlines and the optimization was pushed in the early-stage design process. In this phase, a sub-critical or a super-critical vibration designs can be formulated. Generally, a sub-critical design (all natural frequencies of the system are higher than the highest significant excitation frequency) is preferred. The super-critical design is more exigent and requires verification by the response calculations (Asmussen, 2001).

Thereby, the research work covers analytical vibration modeling of 3D beam structures and 3D stiffened shells (orthotropic panel), as well as the finite element analyses necessary to validate and asses the limitation of the method. This modeling allows to easily taking into account the concentrated masses distributed on the panel surface. The numerical model constituted the base of a vibration module written in FORTRAN. Due to analytical formulation, the vibration module can be effortlessly implemented under an EF code through external subroutines (i.e. UVARM user variables routines in ABAQUS).

NUMERICAL MODEL

Analytical method and particularities

The analytical method is based on the elastic, homogeneous and isotropic material hypothesis. The Euler-Bernoulli formulation assumes that cross-section, which are initially plane and perpendicular to the axis of the beam, remain plane and perpendicular to this axis. The transverse shear deformation is thereby neglected.

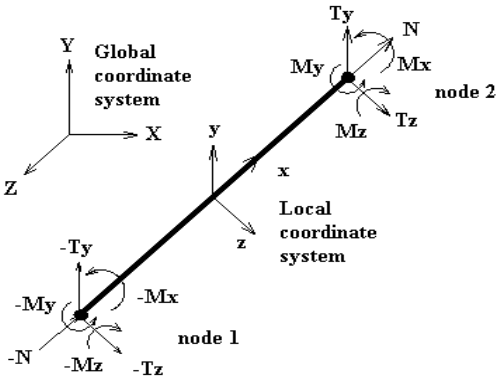

Fig. 1 – Efforts and sign convention for a single beam

Considering the dynamic equilibrium of an elementary section of a beam (Fig. 1), we obtain the next equations of motion for the three fundamental cases, axial, flexural and torsional respectively (Thomson, 1981), Eqs. 1~3. The torsion and the flexion are uncoupled in this study.

$$-\rho A\frac{\partial^2 u}{\partial t^2}+\frac{\partial}{\partial x}\left(EA\frac{\partial u}{\partial x}\right)=0 \tag{1}$$

$$\rho A\frac{\partial^2 v}{\partial t^2}+\frac{\partial^2}{\partial x^2}\left(EI\frac{\partial^2 v}{\partial x^2}\right)=0 \tag{2}$$

$$-\rho I_p\frac{\partial^2 \theta}{\partial t^2}+\frac{\partial}{\partial x}\left(GJ\frac{\partial \theta}{\partial x}\right)=0 \tag{3}$$

where u is the axial displacement, v is the transversal displacement and θ is the angular rotation (twist). A represents the cross-section area, I is the second moment of area, Ip is the polar second moment of area, G the shear modulus and J is the torsional constant.

Since the system is supposed undamped, we assume that a mode of vibration is harmonic, as for discrete systems. Thus the general solution of Eqs. 1~3 is one of the form:

$$h(x,t)=\phi(x)\sin(\omega t+\Psi) \tag{4}$$

where h is the displacement or rotation, ω is the pulsation, Ψ a constant and $\Phi(x)$ an eigenfunction, which describe the mode shape at the frequency ω. Substituting Eq. 4 in the previous equations and factoring out the sine terms, we get the next solutions in axial, flexural and torsional cases respectively:

$$U(x)=A_1\sin(a\,x)+A_2\cos(a\,x) \tag{5}$$

$$V(x)=B_1\sin(b\,x)+B_2\cos(b\,x)+B_3\sinh(b\,x)+B_4\cosh(b\,x) \tag{6}$$

$$\Theta(x)=C_1\sin(c\,x)+C_2\cos(c\,x) \tag{7}$$

where $a=\omega\rho/E$ (pulsation multiplied by the velocity of propagation of extensional waves in the beam), $b=\sqrt{\omega^2\,\rho A/(E\,I)}$ and $c=\omega\sqrt{\rho\,Ip/(G\,J)}$. In theory, the constants A, B, C are evaluated using the boundary conditions. Knowing the displacements and rotation expressions, we can calculate the internal nodal forces in the nodes of the beam by the next formulae, for normal and transversal efforts, and torque and bending moments respectively, Eqs. 8~10.

$$N=EA\frac{\partial U(x)}{\partial x} \tag{8}$$

$$T=-EI\frac{\partial^3 V(x)}{\partial x^3} \tag{9}$$

$$M_\theta=GJ\frac{\partial\Theta(x)}{\partial x}\ \text{and}\ M=EI\frac{\partial^2 V(x)}{\partial x^2} \tag{10}$$

For a single beam (Fig. 1) it is possible to eliminate the constants in order to obtain an expression between nodal local forces (F^L, six per node) and nodal local displacements (U^L, six per node), Eq. 11.

$$\left[F^L\right]_{12x1}=\left[K^L\left(\omega,C_{mp}\right)\right]_{12x12}\left[U^L\right]_{12x1} \tag{11}$$

where C_{mp} represents the mechanical and physical characteristics of the beam.

The matrix K^L represents the stiffness and mass matrix. It is considered a continuous matrix because a beam represents in this case a continuum system. A continuous system has its mass, elasticity and damping distributed. Therefore its mass is inseparable from the elasticity of the beam. In this way, this matrix [$K^L(\omega, C_{pm})$] cannot be decomposed into a separate mass matrix and a separate stiffness matrix without losing in accuracy. This matrix is non-symmetrical and the pulsation ω is located inside the *sin*, *cos*, *sinh* and *cosh* functions.

In the case of a 3D multi-beam structure, the nodal local efforts and displacement must be projected into a global coordinate system. A global continuous stiffness and mass matrix will be obtained. This matrix connects the global nodal effort with the global nodal displacements and allows us to calculate the eigenfrequencies of the system:

$$\left[F^G\right]_{dof\ x\ 1}=\left[K^G\left(\omega,C_{mp}\right)\right]_{dof\ x\ dof}\left[U\right]_{dof\ x\ 1} \tag{12}$$

where "*dof*" represents the total number of degrees of freedom. In reality the resonant phenomena express by very important structural displacements, but numerically the displacements is supposed to tend towards the infinite one. This condition is accomplished by the cancellation of the determinant of the matrix K^G, Eq. 13.

$$\det\left(\left[K^G\left(\omega,C_{mp}\right)\right]_{dof\ x\ dof}\right)=0 \tag{13}$$

Calculating this determinant, an equation function of the pulsation ω (or function of the frequency f) is obtained. The solutions of this equation represent the eigenfrequencies of the beam structure. The total number of the natural frequencies is equal to the degree of the characteristic equation, Eq. 13.

Knowing the external forces acting into the nodes structure, form the Eq. 13 we can obtain the vibrational displacements of each node. For harmonic excitations (at frequencies different from resonant frequencies), the vibrational parameters are connected through the following relations, Eq. 14

$$v = 2\pi \cdot f \cdot s \text{ and } a = 2\pi \cdot f \cdot v \tag{14}$$

Concentrated masses

The beam modeling can easily take into account the concentrated masses on the stiffened panel surface. The masses must be distributed into the beam structure nodes. The presence of these auxiliary masses will determine a decrease of the eigenfrequencies values because the pulsation ω is proportional to the square root of *k/m* (stiffness/mass). To implement the concentrated masses into the vibration calculus, we write the dynamic equilibrium for each node that has an associated mass. We obtain:

$$\begin{aligned} \left[F^G\right] &= \left[K^G\left(\omega, C_{mp}\right)\right]\left[U(x)\right] \\ \left[F^G\right] &= F_{dynamic}\left(= m\ddot{U}(x,t)\right) \end{aligned} \tag{15}$$

where $F_{dynamic}$ are the dynamic inertial forces dues to the concentrated masses. Numerically $F_{dynamic}$ is represented by a diagonal matrix. Considering a harmonic function of time for the displacements, the above relation become:

$$\left(\left[K^G\left(\omega, C_{mp}\right)\right] - \omega^2\left[M_a\right]\right)\left[U(x)\right] = 0 \tag{16}$$

where $[M_a]$ is the additional mass matrix. To calculate the eigenfrequencies of a beam structure with additional masses, we compute the determinant of the next expression:

$$\det\left(\left[K^G\left(\omega, C_{mp}\right)\right] - \omega^2\left[M_a\right]\right) = 0 \tag{17}$$

Stiffened panels

To calculate analytically the eigenfrequencies of a stiffened panel we employ a virtual artifice that consists in the decomposition of the panel into a beam grid, as presented in the Fig. 2. The vibration analysis uses then the beam model already described.

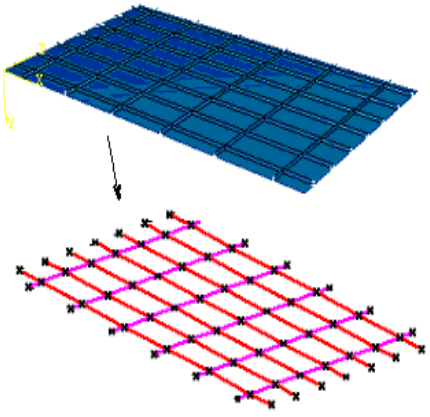

Fig. 2 – Decomposition of a stiffened panel into a beam grid

This choice allows us to use the beam theory to solve the problem. At the same time it will be easily to assess vibration for complex structures like stiffened panels - beams assemblies and also to take into account concentrated masses distributed on the panel surface.

The mass of the plate (without stiffeners) will be distributed along the longitudinal stiffeners in order to keep the beam aspect approximation. The main condition is to preserve the global inertia of the stiffened panel and total mass of the structure. For stiffened panels having only one direction stiffeners, the mass of the plate will be distributed on the second direction (perpendicularly on stiffeners) by creating virtual beam on this direction.

After the split of the stiffened panel into a beam grid, it is necessary to calculate the second moment of area of each beam section of the new structure. The second moment of area about y-axis I_y is calculated with respect to the vertical principal axis of the considered cross section (Fig. 3).

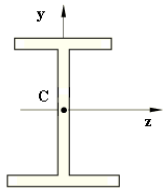

Fig. 3 – Notations of transversal cross-section

To calculate the second moment of area about z-axis I_z, we define three feasible cases. For the first case, this parameter is defined with respect to the horizontal principal axis of the considered section. This axis pass through the barycenter of the beam section for each beam, noted C1 on Fig. 4.

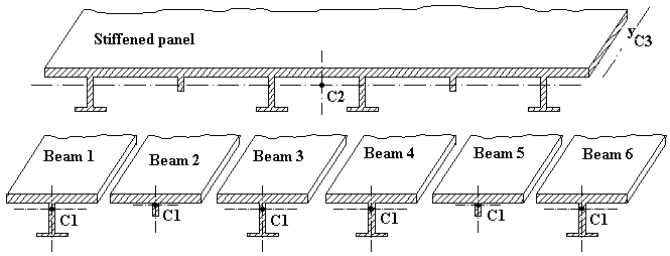

Fig. 4 – Decomposition of a transversal side of a panel into beams

In the second case, I_z is calculated with respect to the horizontal principal axis of the undivided section of the stiffened panel, passing through the barycenter (noted C2 for transversal section and C3 for longitudinal section) of the entire side, Fig. 4. Therefore, after the decomposition of a side of the panel into beams, all parameters I_z are calculated with respect to the same axis. This position of this axis on the ordinate Oz may be different for transversal and longitudinal cases. For the third case, all I_z of transversal and longitudinal sections are calculated with respect to the axis passing through the virtual centroid C_z of the whole stiffened panel. The position of this point on the ordinate Oz is given by the Eq. 18.

$$C_z = \left(z_c{}^T \cdot A^T + z_c{}^L \cdot A^L\right) / \left(A^T + A^L\right) \tag{18}$$

where $z_c{}^T$ and $z_c{}^L$ are the centroid (C) of the transversal and horizontal cross-section area of the entire stiffened panel, and A^T and A^L the correspondents cross-section areas.

CPU time dissemination

The resolution of the Eq. 13 and Eq. 16, where the unknown is the pulsation, makes it possible to find the eigenfrequencies of the beam structure. Numerically, two methods were tested.

The first method supposes to divide the relevant frequency interval into small fixed intervals and calculate the determinant at each frequency step. A change of the determinant sign indicates a solution of the characteristic equation. The accuracy of this method is influenced by the frequency step dimension, but smaller is the step larger is the CPU calculation time. We have tried 5 common numerical methods to calculate the determinant of the global mass and stiffness continuous matrix, Eq.13. The Table 1 summarizes the CPU time machine necessary to find the first natural frequency of a beam structure with 300 degrees of freedom. The program carries out 37 calculations of the determinant (frequency range from 0.1 Hz to 3.7 Hz with an increment of 0.1 Hz, the first eigenfrequency being between 3.6 Hz and 3.7 Hz).

Table 1. Numerical methods used to calculate the determinant of a matrix

Method (single precision)	CPU time
Leverrier algorithm	hours
Product of eigenvalues (Lapack)	57.00 s
Gauss partial-pivoting scheme	14.9 s
Classic LU decomposition	11.5 s
Optimized LU decomposition (Lapack)	7.9 s

The optimized LU decomposition using Lapack libraries of linear algebra routines proves to be the fastest method with 0.21 seconds per increment for this case. Using the same method, for a beam structure with 990 dof, the time was around 1 s per increment (on a laptop with Intel Centrino Core 2 Duo T7300 2 GHz, 4 GB DDR2 RAM). All methods give identically results.

The second method supposes to dissociate the matrix $K^G(\omega, C_{mp})$ into a mass matrix $M^G(C_{mp})$ and a static stiffness matrix $K^G(C_{mp})$, similar to the discrete systems. To obtain the static stiffness matrix, we carry out series expansions at least 15 terms of the matrix $K^G(\omega, C_{mp})$ and of his double derivation with regard to ω in the vicinity of $\omega = 0$.

$$K^G(C_{mp}) \cong \lim_{\omega \to 0} K^G(\omega, C_{mp}) \tag{19}$$

$$M^G(C_{mp}) \cong -\frac{1}{2} \lim_{\omega \to 0} \frac{\partial^2 K^G(\omega, C_{mp})}{\partial \omega^2} \tag{20}$$

These matrices are independents of the frequency *f*. With this approach, the resonant frequencies are obtained solving the eigenvalue problem, Eq. 21.

$$K^G - \omega^2 M^G = 0 \tag{21}$$

The CPU time is considerably reduced: 1.4 s instead 7.9 s for the case characterized by 300 dof.

The last method represents an approximation of the analytical method and it is valid for the lower frequency domain (< 100 Hz). For a simple analysis, the first method is more relevant but is not the case for the optimization software that requires very small CPU time. In this case, the second method shall be used.

TESTS AND RESULTS

3D beam structures

The first validation of the vibration tool was realized on 3D beam structures. The finite element simulations used a beam modeling. For both simulations (FE and vibration tool), all connected nodes are rigidly joined, instead all non-connected nodes are clamped. All the beam sections are identically. We have treated two typical of structures, i.e. a 3D type (masts,
Fig. 5) and a planar type (planar grid, Fig. 6). The material is steel (E = 2.1e11 N/m^2, ρ = 7800 kg/m^3, ν = 0.3).

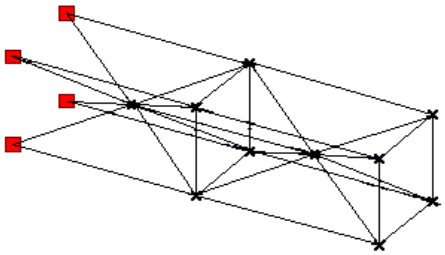

Fig. 5 – First problem test - 3D multi-beam structure, length 24 m, width = 6 m, annular section (Φ = 100 mm, thickness = 10 mm)

Table 2. First problem test results

Method (single precision)	Frequency			
	f_1	f_2	f_3	f_4
Classic dichotomy	0.76	1.40	-	-
Discrete method	1.24	1.35	1.50	1.61
ABAQUS	0.52	1.47	3.09	3.20

Generally, only FE calculus using very fine mesh can supply results closed to those of analytical continuum methods. Using classic dichotomy method, the natural frequencies agree well with those determined with ABAQUS, Table 2. The differences can be justified by unheeded of the constrained torsion. Moreover, we don't use the Timoshenko's beam model, so we neglect shear and rotational inertia effects. The results obtained with discrete method are different. This second method is adapted for complex three-dimensional structure only using many beams and many beam connections.

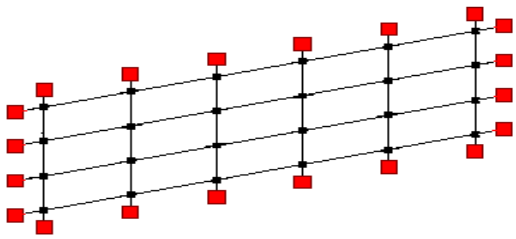

Fig. 6 – Second problem test - Planar beam structure, length 17 m,

width = 8 m, rectangular section (h = 30 mm, b = 40 mm)
The Table 3 present the results obtained with classic dichotomy method, discrete approach and ABAQUS for the second problem test. For planar structures the both numerical methods give practically the same results, but with different CPU times (greater for the classic dichotomy). These results are also in good correlation with ABAQUS results.

Table 3. Second problem test results

Method (single precision)	Frequency		
	f_1	f_2	f_3
Classic dichotomy	1.55	2.15	2.68
Discrete method	1.56	2.16	2.80
ABAQUS	1.72	2.22	3.15

3D stiffened panels

The second validation of our vibration module uses planar stiffened panels. The first type of tested problems refers to stiffened panels with clamped edges. We consider the rectangular panel (20 x 30 x 0.006 m) represented in the Fig. 7. It has 11 identical transversal frames (T section, web 0.25 x 0.01 m, flange 0.2 x 0.012 m) and 15 different longitudinal frames (the same T section and L section - web 0.16 x 0.008 mm, flange 0.05 x 0.02 m). The material is steel (E = 2.1e11 N/m^2, ρ = 7850 kg/m^3 and ν = 0.3).

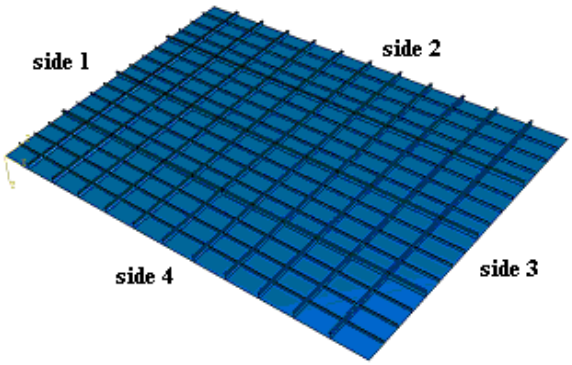

Fig. 7 – Third problem test - complex stiffened panel

Table 4. Third problem test results

Boundary condition	Freq. Hz	Vibration tool			ABAQUS
		Case 1	Case 2	Case 3	
BC1	f_1	3.99	4.02	4.02	3.89
	f_2	5.34	5.46	5.46	5.31
	f_3	8.29	8.59	8.55	8.15
BC2	f_1	0.60	0.60	0.60	0.60
	f_2	1.35	1.40	1.40	1.33
	f_3	2.84	2.85	2.85	3.20
BC3	f_1	1.16	1.21	1.22	1.09
	f_2	1.31	1.37	1.37	1.27
	f_3	2.87	2.87	2.87	2.88

For this problem, we apply three different boundary conditions on free edges:
- BC1 – all sides clamped;
- BC2 – sides 1 and 2 clamped, sides 3 and 4 free;
- BC3 – sides 1 and 3 clamped, sides 2 and 4 free.

The value of the second moment of area about z-axis I_z is calculated with respect to the three axis already discussed, i.e. the principal axis of the considered section (case 1), principal axis of the undivided section of the stiffened panel for each side (case 2) and the axis passing through the virtual centroid C_z of the whole stiffened panel (case 3) respectively. The classic dichotomy and discrete approachesh give the same results, but with bigger CPU times fir the first method. All results presented in the Table 4 are in good agreement with those of ABAQUS, but those of case 1 (second moment of area about z-axis I_z is calculated with respect to) are much closed. However, the vibration tool results remain higher than ABAQUS results.

The second type of studied problems relates to platforms. The boundary conditions impose to block the displacements and rotations for 4 nodes, Fig. 8. The panel (4 x 3 x 0.016 m) has identical transversal and longitudinal frames disposed symmetrically. The section of the frames is I profile with web 50 x 10 mm and no flange. The material is steel.

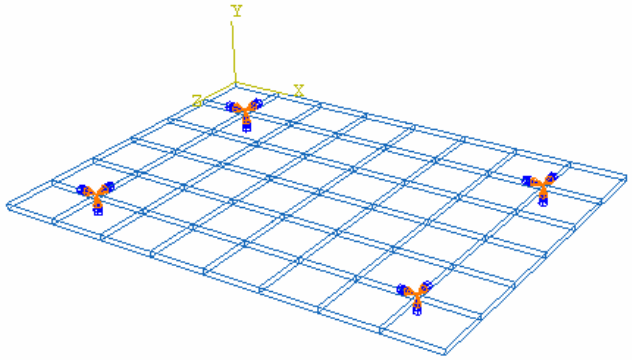

Fig. 8 – Forth problem test - complex stiffened panel

Table 4 gives the results obtained with our numerical tools (classic dichotomy method and the discrete approach) and those of ABAQUS. In this case, the panel and the stiffeners are meshed with shell elements.

Table 5. Forth problem test results

Method (single precision)	Frequency			
	f_1	f_2	f_3	f_4
Classic dichotomy	8.52	10.52	13.67	18.52
Discrete method	8.54	10.52	13.73	18.59
ABAQUS	8.67	10.59	17.53	19.21

Excepting the mode 3, the numerical tool results are in very good agreement with ABAQUS results. In ABAQUS, all 4 modes are global modes of vibration. Unfortunately, we can only to compare the natural frequency values. To view the vibration mode associate to each natural frequency, we must model under an FE code the equivalent beam grid associate to considered panel. Our simulations using the equivalent beam grid ensure that the first modes are global modes.

Vibration module limitations

As we have already described, the vibration tool uses a beam modeling. As a consequence the deformation of the shell between beam grid cannot be take into account. If the beams of the panel have a very high moment of inertia, the first vibration modes are represented by local modes, as presented in Fig. 9. If the stiffeners' width is very large the first mode of vibration can also be a local mode. Certainly, the boundary conditions can also affect the vibration modes.

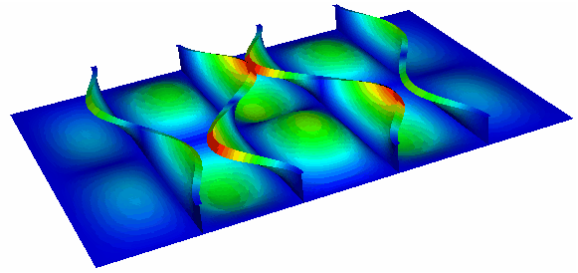

Fig. 9 – Local vibration modes of a stiffened panel

To identify some limitations of this numeric tool, we tested a particular type of stiffened panel in relevant configurations.

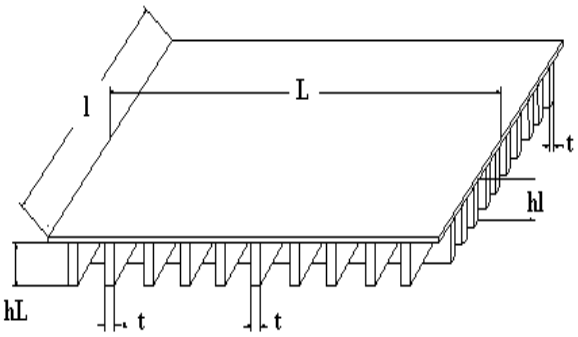

Fig. 10 – Stiffened panel notations

The first three configurations refer to a square panel, and the next five configurations refer to a rectangular panel. The both structures have 10 transversal and 10 longitudinal stiffeners. The stiffeners are disposed symmetrically with respect to the symmetry axis of the panel and the distance between them is equally. Fig. 10 and Table 6 present the characteristic dimensions of each case.

Table 6. Panel dimensions

Case	L	l	hL	hl	t
1	6.6 m	6.6 m	0.22 m	0.22 m	8 mm
2	6.6 m	6.6 m	0.44 m	0.22 m	8 mm
3	6.6 m	6.6 m	0.66 m	0.22 m	8 mm
4	19.8 m	6.6 m	0.22 m	0.22 m	8 mm
5	19.8 m	6.6 m	0.44 m	0.22 m	8 mm
6	19.8 m	6.6 m	0.66 m	0.22 m	8 mm
7	19.8 m	6.6 m	0.22 m	0.44 m	8 mm
8	19.8 m	6.6 m	0.22 m	0.66 m	8 mm

Concerning the results, we compared our results with those of COSMOS only for the first global mode of vibration, Table 7. Apart from the cases 3 and 8 for which the first mode of vibration is a local mode (vibration of stiffeners), all other results are in good concordance.

Table 7. Natural frequency and modes

Case	First natural frequency Hz		Mode
	Vibration tool	COSMOS	
1	32.08	30.10	1
2	56.97	53.36	1
3	86.43	77.21	111
4	15.41	15.40	1
5	14.96	15.15	1
6	15.83	15.77	1
7	39.09	34.89	1
8	62.86	53.01	87

It is very difficult to give the real limitations of this vibration tool. After few tests, we consider that the dimensions of the stiffeners must remain smaller in front of the dimension of the shell and the distance between stiffeners.

CONCLUSIONS

In this paper, a numerical approach to calculate the resonant frequencies for beam structures, stiffened panels and their assemblies is presented. Finite element simulations were carried out to validate the numerical tool.

Two methods can be used to obtain the natural frequencies. The first, named classic dichotomy is based on Euler-Bernoulli equations and is purely analytical. In this case it is necessary to divide the relevant frequency interval into small intervals and to calculate the determinant of the characteristic mass and stiffness continuum matrix. The main advantage of this method is the accuracy of the results. Nevertheless, this accuracy is limited by the modeling and is influenced by frequency step size. The main inconvenience is the large CPU calculation time in case of complex structures (over 600 dof). In some cases, the numerical tool delivers some parasite frequencies in the vicinity of a natural frequency. This may be due to some numerical errors and/or a non-dimensionless model. To integrate the numerical model into an optimization design process (that requires reduced CPU calculation time) a second method, named discrete approach, was developed. The calculation time becomes very small even for structures with many degrees of freedom (2000 dof) and the parasite frequencies disappear. This method was validated with simplified FEA (beam mesh which contains only one element).

The numerical model constituted the support of a vibration module written in FORTRAN. The module was transformed into a DLL for which the input data is represented by all dimensions of the panel (plate and stiffeners), the positions of the stiffeners on the plate, the mechanical and physical characteristics, and the boundary conditions of the exterior sides of the panel. The eigenfrequencies of the stiffened panel represent the output data. The vibration module is fully automatically because, from the input data, it is capable to split the stiffened panel into beams realizing a correct distribution of the masses,

to calculate the mechanical parameters (second moments of area) and to apply the boundary conditions.
Due to beam modeling, the both methods allow to obtain only the resonant frequencies corresponding to global vibration modes. The modeling of the concentrated masses was tested and validated only in the case of simple structures.

In practical dimensioning, the two first natural frequencies are the most relevant. These two values calculated with the vibration tool are very close to those given by ABAQUS for all problems treated in this paper. In conclusion, taking into account the limitations of these methods, it is appreciated that the numerical tool can be successfully used to calculate correctly at least the two first resonant frequencies for beam structures and stiffened panels.

ACKNOWLEDGEMENTS

We are grateful for discussions and simulation results of Prof. I. Chirica (SDG, Galati, Romania) and to University of Liege (Belgium) for the Post-doctoral Fellowship. The research has been performed under the 6th Framework Programme (MARSTRUCT FP6-PLT-506141 and IMPROVE FP6-031382 EU Projects).

REFERENCES

Asmussen, I., Menzel, W., and Mumm, H. (2001). "*Ship Vibration*", Germanischer Lloyd

Jia, J. (2008). "*Numerical and Experimental Investigation of Dynamics of Vehicle/Ship-Deck Interactions", Marine Technology*, Vol. 45, No. 1, pp. 28-41

Thomson, W. (1981). "*Theory of Vibration with Applications"*, Prentice-Hall, Inc.